Supplementary Information

Scalable Synthesis of CuSn Bimetallic Catalyst for Selective CO$_2$ Electroreduction to CO over a Wide Potential Range

Zi-Chun Zhu [a, c#], Jun-Yan Ge [a, c#], Man Qiao [b#], Xue-Li Yang [a], Yu-Jia Tang [b], Dongdong Zhu [b,*], and Ping Chen [a,*]

[a] School of Materials Science and Engineering, Anhui University, Hefei, Anhui, 230601, China.

E-mail: chenping@ahu.edu.cn

[b] School of Chemistry and Materials Science, Institute of Advanced Materials and Flexible Electronics (IAMFE), Nanjing University of Information Science and Technology, Nanjing, 210044, China.

E-mail: dd.zhu@nuist.edu.cn

[c] School of Materials and Environment Engineering, Chizhou University, Chizhou, Anhui, 247000, China.

[#]These authors contributed equally to this work.

1. Experimental Section

1.1 Catalyst Synthesis.

Typically, a self-supported CuSn bimetallic catalyst was prepared on carbon paper by industrial electroplating following by simple annealing treatment, and quick in-situ electroreduction. Firstly, Cu was electroplated on a carbon paper ($2.5*2$ cm^2) by a typical two-electrode configuration under ambient conditions. In detail, carbon paper was used as cathode and platinum sheet was used as anode. The electroplating solution contained $CuSO_4$, H_2SO_4 and light agent. A current of 0.1 A was applied for 5 min. Then, Sn was electroplated onto the above product using the electroplating solution containing methyl sulfonate and tin methyl sulfonate with the volume ratio of 1:1. A voltage of 1.0 V was applied for 1 min. The products were then put into a tube furnace and calcined in air at 500 °C for 2h. The heating rate is 1 °C min^{-1}, and the cooling rate is 5 °C min^{-1}. Finally, the product was obtained by electrochemical reduction in Na_2SO_4 solution for 10 min and then directly used as cathode for CO_2 reduction.

The preparation of the self-supported Cu catalyst on carbon paper was similar to that of CuSn bimetallic catalyst, but without the process of Sn electroplating.

The preparation of the self-supported Sn catalyst on carbon paper was similar to that of CuSn bimetallic catalyst, but without the process of Cu electroplating, and the electroplating time of Sn was 5 min.

The preparation of the self-supported CuIn bimetallic catalyst on carbon paper was similar to that of CuSn bimetallic catalyst, and it contained Cu electroplating, and

then In electroplating steps. In the process of In electroplating, the plating solution contained 10.0 mM $InCl_3$ and 2.0 mM NaCl. A voltage of 1.1 V was applied for 20 min.

1.2 Material characterization.

The morphologies of the products were characterized by a scanning electron microscope (SEM, HITACHI Regulus 8230, Japan), and a field emission transmission electron microscope (JEOL JEM 2100, Japan). The crystal phase of the products was characterized by a powder X-ray diffraction (XRD patterns, Rigaku SmartLab 9KW with Cu-kα radiation, λ=0.15406 nm) from 10 to 80° with a rate of 10° min^{-1}. XPS data of the products were obtained using a Thermo ESCALAB 250Xi X-ray photoelectron spectrometer (Thermo ESCALAB 250Xi, USA).

1.3 Electrochemical measurement and product analysis.

All electrochemical experiments were performed in an H-type electrochemical cell, which contained two compartments separated by a Nafion 117 membrane. Each compartment had 50 mL electrolyte (0.5 M $KHCO_3$) and about 50 mL headspace. A three-electrode system was used to investigate the electrocatalytic CO_2 reduction activity of the catalysts by a CHI760D electrochemical workstation at room temperature. In the system, a Pt plate and Ag/AgCl electrode were used as counter and reference electrodes, respectively. The as-fabricated bimetallic catalyst on carbon paper was used as a working electrode. Before measurement, the cathodic compartment was degassed and saturated with high-purity CO_2 (99.999%) at 40 mL

min[-1] for at least 20 min. In the reduction process, CO_2 gas was continuously bubbled into the cathodic chamber at the rate of 40 mL min^{-1}. All potentials were investigated against an Ag/AgCl reference electrode and converted to reversible hydrogen electrode (RHE) potentials without iR compensation. An on-line gas chromatograph (GC) equipped with a flame ionization detector (FID) and a thermal conductivity detector (TCD) was used to measure the gas samples. The liquid products were measured by a nuclear magnetic resonance (NMR, Bruker 400 MHz). We collected the product data for three times at each fixed potential, then the average results are obtained and used.

1.4 Computational methods.

First-principle DFT calculations were carried out using the plane-wave technique in the Vienna ab initio simulation package (VASP).[1,2] The projector augmented wave (PAW) approach was used to describe the ion-electron interaction.[3] The generalized gradient approximation (GGA) involving the Perdew-Burke-Ernzerhof (PBE) functional was adopted to describe the exchange-correlation interactions.[4] A converged cutoff energy of 420 eV with Fermi-level smearing of 0.1 eV for surfaces and 0.01 eV for gas-phase species was used in our calculations. The Grimme's D3 van der Waals correction was employed to treat the long-range vdW interactions.[5] The Cu (211) plane was chosen as the active surface, because that stepped facets are generally more active than flat terrace sites toward CO_2 electroreduction.[6] The structure of pure Cu and CuSn bimetallic catalysts were modeled with a six-layer (2×4) Cu(211) slab, of which only the top three layers are allowed to relax. It should

be noted that we model the CuSn bimetallic catalyst with one Sn atom in place of the exposed Cu atom in the outer layer, since it has a smaller substitution energy than the inner layer. The Brillouin zone was sampled with $11\times11\times11$ k-points for bulk calculations and $3\times3\times1$ k-points for surface calculations. The convergence threshold was conducted as 10^{-4} eV in energy and 0.05 eV/Å in force, and a vacuum region of around 15 Å was set along the z-direction to avoid the interaction between periodic images.

For CO_2 electroreduction, the free energy (G) of each adsorbate was calculated by

$$G = E_{DFT} + E_{ZPE} + \int C_p dT - TS$$

where E_{DFT}, E_{ZPE}, C_p, S and T were the electronic energy, zero point energy, heat capacity, entropy, and temperature (298.15 K), respectively. For adsorbed species, the E_{ZPE}, C_p and S were obtained by vibrational frequencies calculations with harmonic approximation and neglect of contributions from the slab. For molecule, those values were taken from the NIST database.[7] These contributions are listed in Table S1. The solvent effect on adsorbates was achieved using the Poissson-Boltzmann implicit solvation model with a dielectric constant of 80.[8]
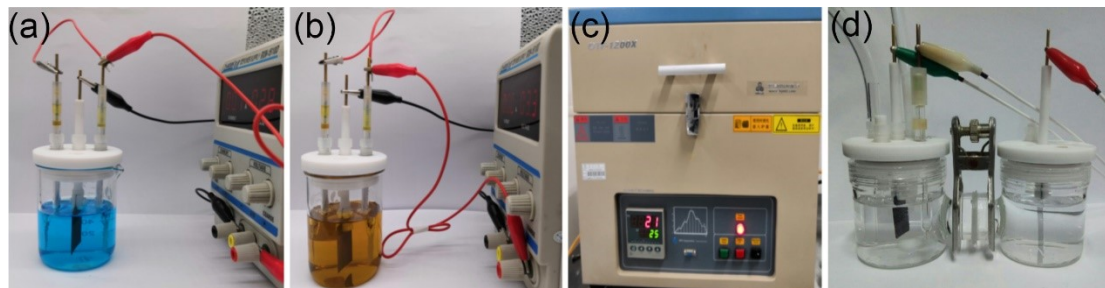
2. Supplementary Figures and Tables

Figure S1. Schematic illustration showing the synthesis process of CuSn on carbon paper, which includes four subsequent steps: (a) Cu electroplating, (b) Sn electroplating, (c) annealing treatment, and (d) final *in situ* electroreduction.
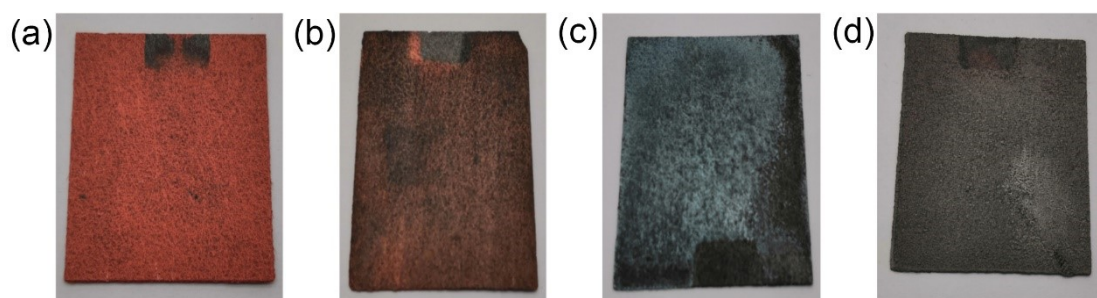

Figure S2. Photographs of the samples obtained after (a) Cu electroplating, (b) Sn electroplating, (c) annealing treatment, and (d) *in situ* electroreduction, respectively.
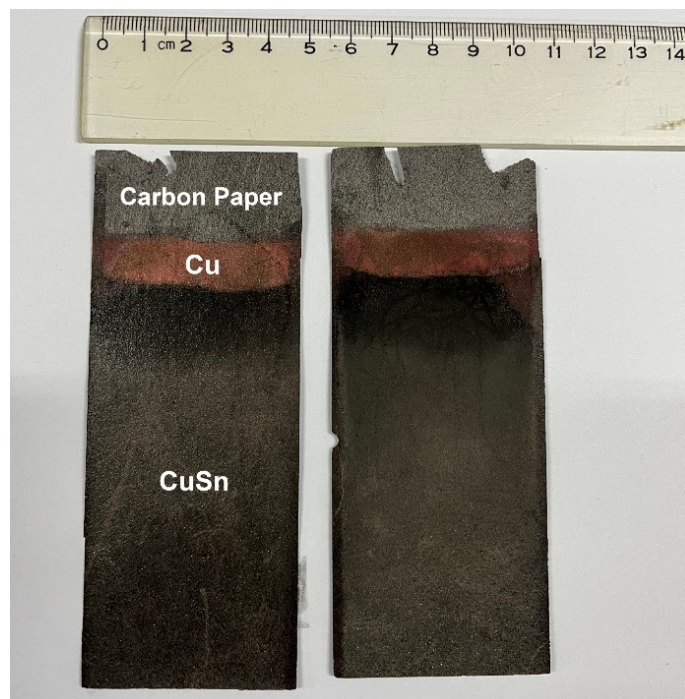
Figure S3. Photograph of the CuSn samples prepared on carbon paper with larger sizes, demonstrating the scalability of the material preparation method.
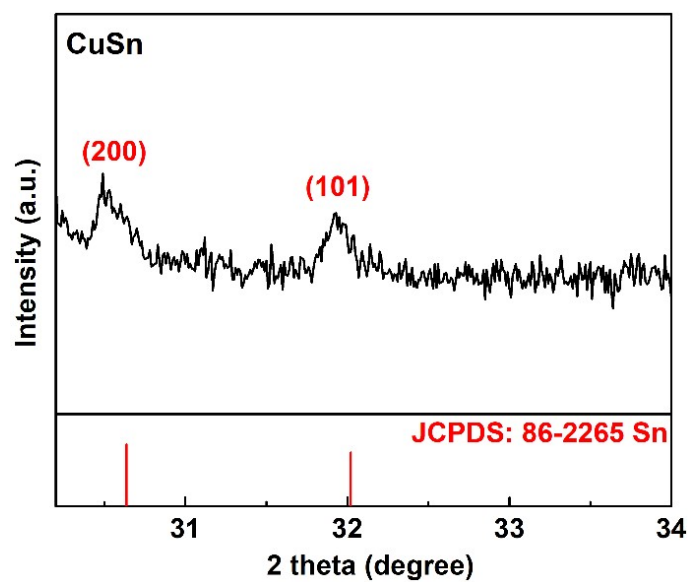

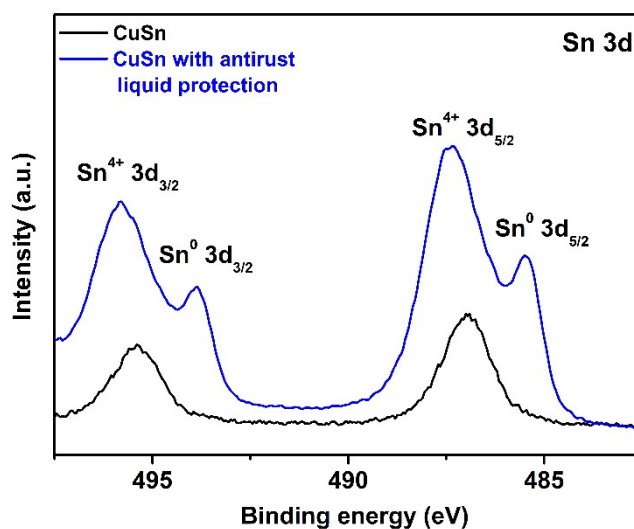Figure S4. The enlarged XRD pattern of CuSn sample.

Figure S5. Sn 3d XPS spectra of the CuSn samples with or without antirust liquid protection.

Sn^0 species were observed in CuSn sample with antirust liquid protection, while only Sn^{4+} species exist in CuSn sample without antirust liquid protection, suggesting that the oxidized species can be attributed to the surface oxidation of the sample in ambient conditions.
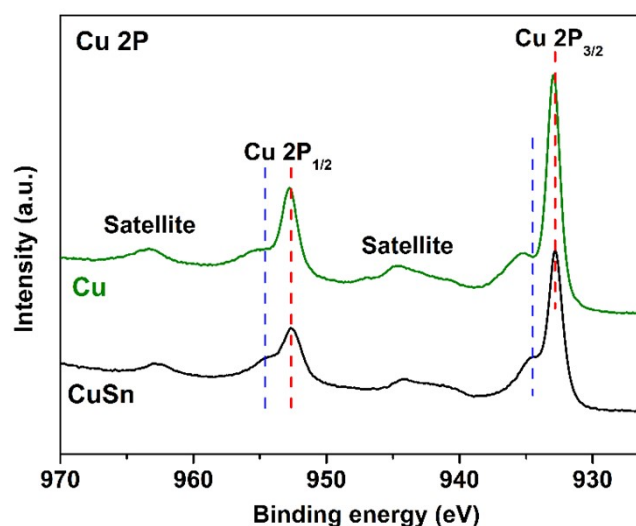

Figure S6. Cu 2p XPS spectra of CuSn, and Cu samples.

Compared to Cu sample, all the Cu 2p peaks of CuSn shift noticeably to lower binding energies, indicating that electrons transfer from Sn to Cu (charge redistribution) in the CuSn sample, leading to the generation of Cu species with lower oxidation states.
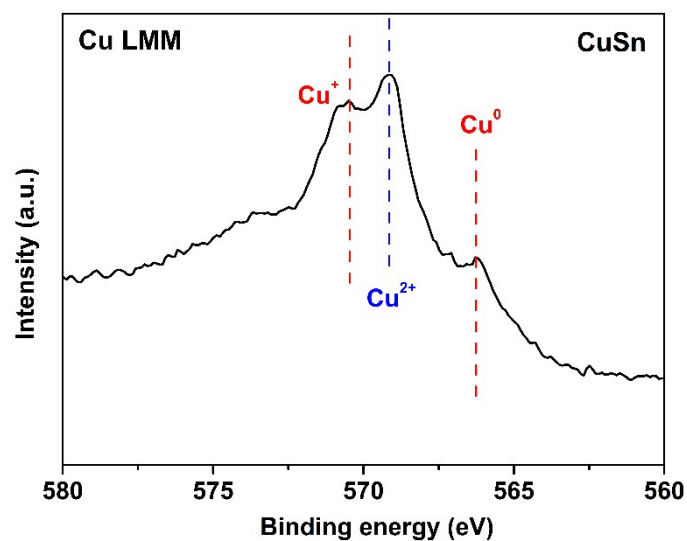
Figure S7. Auger Cu LMM XPS spectrum of CuSn samples.

Besides Cu^{2+} peak positioned at 569.1 eV, another two peaks located at 570.4 and 566.3 eV are well assigned to Cu^+ and Cu^0 peaks (J. Am. Chem. Soc. 2019, 141, 6986), respectively, confirming the existence of Cu^{2+}, Cu^+, and Cu^0 species in the CuSn sample.

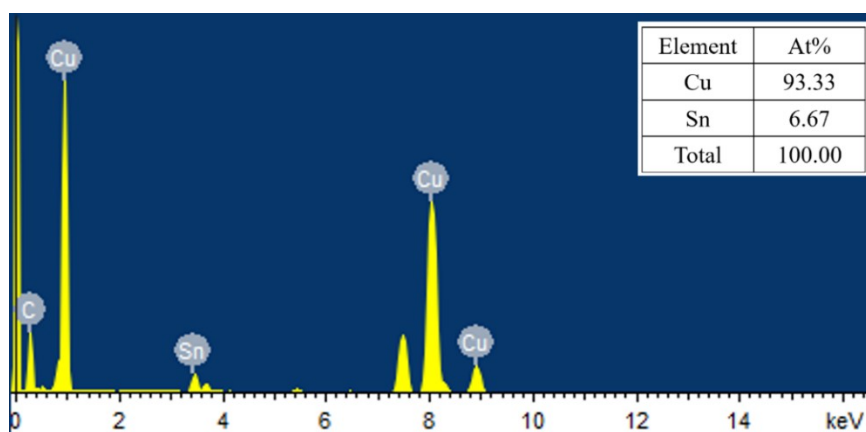| Element	At%
Cu	93.33
Sn	6.67
Total	100.00

Figure S8. Transmission electron microscopy energy dispersive X-ray spectroscopy (TEM-EDS) spectrum of CuSn. The atomic ration of Cu/Sn is 14:1.
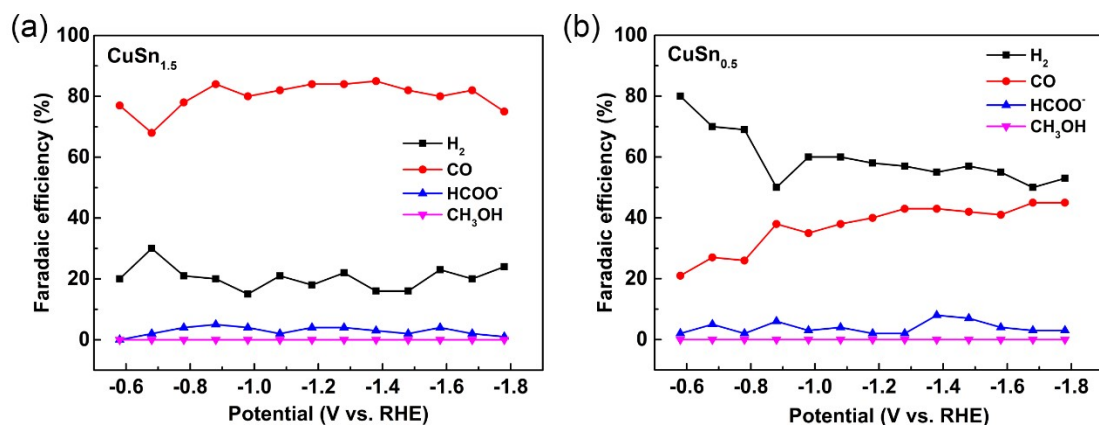
Figure S9. Potential dependence of Faradaic efficiencies for CO_2 electroreduction on CuSn samples with different Sn electroplating time of (a) 1.5 mins, and (b) 0.5 min, respectively.
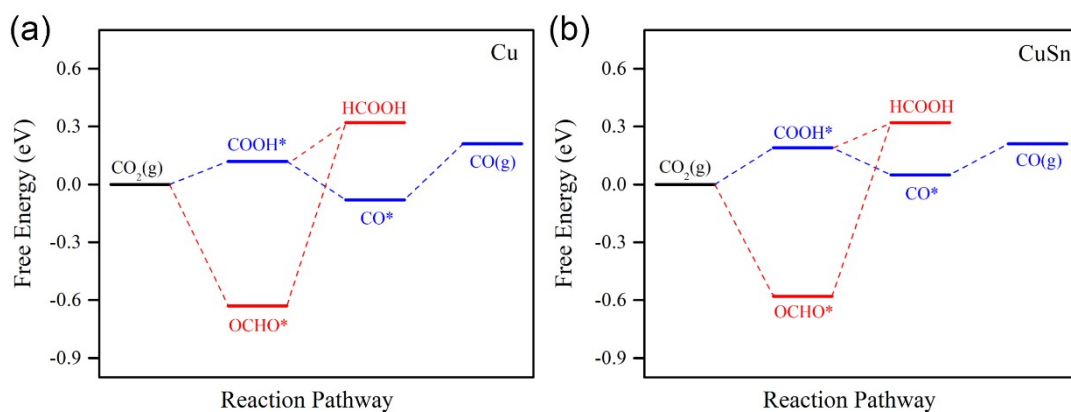

Figure S10. Free energy profiles of pathways for CO_2 electroreduction to CO and HCOOH on (a) Cu, and (b) CuSn.
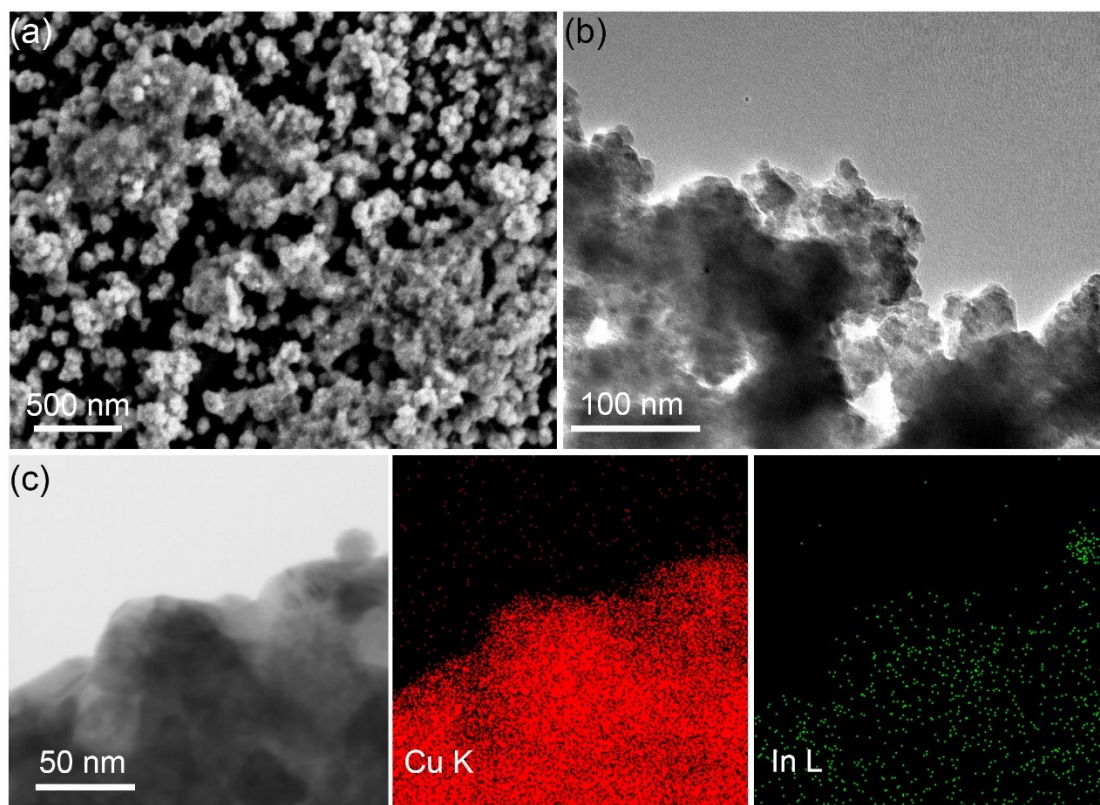
Figure S11. (a) SEM image of CuIn. (b) TEM image of CuIn. (c) HAADF-STEM image and the corresponding elemental mapping of CuIn.
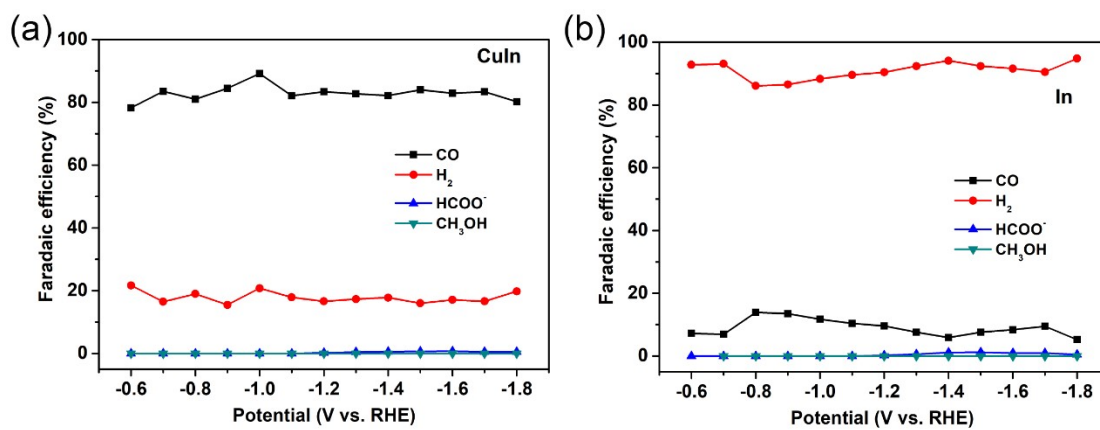

Figure S12. Potential dependence of Faradaic efficiencies for CO_2 electroreduction on (a) CuIn, (b) In.

Table S1. Zero-pint energy correction (E_{ZPE}), entropy contribution (TS), heat capacity, and the total free energy correction ($G - E_{\text{elec}}$) in this study.

Species	E_{ZPE} (eV)	$\int CpdT$ (eV)	$-TS$ (eV)	$G - E_{\text{elec}}$ (eV)
H_2	0.27	0.09	−0.42	−0.06
H_2O	0.57	0.10	−0.69	−0.02
CO	0.13	0.09	−0.61	−0.39
CO_2	0.31	0.12	−0.68	−0.25
HCOOH	0.89	0.09	−0.99	−0.01
COOH*	0.60	0.11	−0.20	0.50
OCHO*	0.61	0.11	−0.23	0.49
CO*	0.18	0.08	−0.13	0.13

References

1. G. Kresse, J. Furthmüller, *Phys. Rev. B* **1996**, *54*, 11169−11186.

2. G. Kresse, J. Furthmüller, *Comput. Mater. Sci.*, **1996**, *6*, 15−50.

3. G. Kresse, D. Joubert, *Phys. Rev. B* **1999**, *59*, 1758−1775.

4. J. P. Perdew, K. Burke, and M. Ernzerhof, *Phys. Rev. Lett.*, **1996**, *77*, 3865−3868.

5. S. Grimme, *J. Comput. Chem.*, **2006**, *27*, 1787−1799.

6. A. A. Peterson, F. Abild-Pedersen, F. Studt, J. Rossmeisl and J. K. Nørskov, *Energy Environ. Sci.*, **2010**, *3*, 1311-1315.

7. Computational Chemistry Comparison and Benchmark Database. http://cccbdb.nist.gov/.

8. K. Mathew, R. Sundararaman, K. Letchworth-Weaver, T. A. Arias, and R. G. Hennig, *J. Chem. Phys.*, **2014**, *140*, 084106.